JOURNAL OF CATALYSIS 66, 229–236 (1980)

The Reduction of Nitric Oxide by Hydrogen over $Pt/\gamma\text{-}Al_2O_3$ as a Function of Metal Loading

K. OTTO AND H. C. YAO

Research and Engineering Research Staff, Ford Motor Company, Dearborn, Michigan 48121

Received March 24, 1980; revised June 11, 1980

The reduction of nitric oxide by hydrogen on platinum, supported on γ-alumina, is evaluated as a function of Pt concentration in the range from 273 to 373 K. Product distribution and apparent activation energy in this temperature range remain rather constant as the Pt atoms change from a dispersed phase to a particulate phase of distinct clusters. Measured per chemisorption site, atoms in the particulate phase are much more reactive than atoms in the dispersed phase. Optimum catalyst efficiency is reached at a Pt loading of about 5 wt%. Theoretical considerations, based on transition state theory, suggest that the dissociation of NO is rate determining.

INTRODUCTION

This work is a continuation of an investigation of catalytic effects that depend on the degree of dispersion of Group VIII noble metals. In a recent publication (*1*) about Rh, supported on γ-alumina, pronounced changes were found in reaction parameters, e.g., rate, activation energy, and product distribution, as the metal loading on the support was varied. More specifically, a distinct change in reaction parameters at a moderate Rh coverage of the support surface confirmed the existence of two catalyst phases on the support. One catalytic species, called the dispersed phase, predominates at low surface concentrations, while the second kind, consisting of three-dimensional clusters, characterizes high loadings. Two distinct catalyst phases were also identified for the case of Pt on γ-alumina by the use of selective chemisorption, temperature-programmed reduction, and transmission electron microscopy (*2*). To explore catalytic changes associated with such a phase change, the reduction of nitric oxide by hydrogen as a function of Pt concentration was studied and the results compared with kinetic data obtained for the case of Rh (*1*). To evaluate the reaction mechanism on a quantitative basis, the experimental densities of Pt sites, as measured by selective chemisorption, were compared with a theoretical reaction-site density, deduced from basic kinetic considerations.

EXPERIMENTAL

The preparation of the γ-alumina support and the deposition of Pt from aqueous solutions onto the support have been described previously (*2*). With one exception, the samples used here were used before to study the interaction between Pt and γ-alumina and to measure the degree of Pt dispersion by selective chemisorption of hydrogen and of carbon monoxide. The samples were initially kept in air at 775 K for 3 hr, then reduced in hydrogen at 575 K and evacuated at 675 K overnight before reaction rates were measured.

A batch reactor containing a recirculation pump (*1, 3*) was used for the reaction studies. The initial mixture contained approximately 85 Torr of NO, 70 Torr of H_2, and 300 Torr of Ar, thus providing overall oxidizing conditions. The sample charge was adjusted before each series of experiments to expose approximately the same amount of Pt (50 μmol) on the support surface. Reaction temperatures were selected in the range from 273 to 373 K. Reaction temperatures below 273 K were avoided because of the problem of ice for-

0021-9517/80/110229-08$02.00/0

mation on the active surface, although NO reduction was measurable even at 250 K. Small samples of the gas mixture were removed during the reaction for analysis by mass spectrometer. The concentrations of nitrogen, nitric oxide, and nitrous oxide were evaluated from the mass peaks at m/e = 28, 30, and 44, after a correction had been applied for the fragmentation pattern of nitrous oxide. The absolute amounts of reactants and products were based on the constant amount of Ar in the mixture. The reduction of nitric oxide to ammonia was determined indirectly from the mass balance of nitrogen. Further details of the experimental setup are given elsewhere (*1, 3*).

RESULTS

Initially reaction rates were measured at a given temperature by monitoring the reaction until completion. The accuracy of the temperature coefficient derived from these rate measurements, however, was unsatisfactory. The reproducibility of the temperature coefficient was improved by a modification of the rate measurement procedure. To this end the reaction rate was measured at one temperature until about one-third of the initial NO had been used up, the temperature was then quickly changed to another value. The time dependence of these rate measurements is illustrated in Fig. 1. The curves were selected to show examples for an abrupt increase (top) and decrease (bottom) in temperature. A temperature coefficient was evaluated at the point of temperature changeover. The reaction rate at this point is measured under corresponding conditions: The amount of NO converted is constant, and the product distribution remains constant for all the samples.

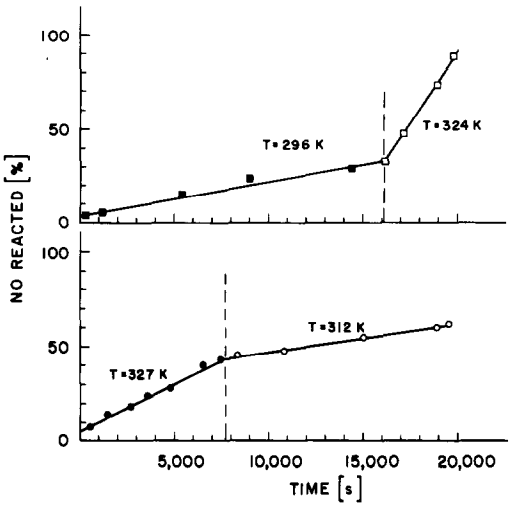

FIG. 1. Reduction of NO by H_2 over Pt: (a) Loading 4.9 wt%, at (■) 296 K and (□) 324 K. (b) Loading 0.78 wt%, at (●) 327 K and (○) 312 K. Initial gas concentration (in Torr): NO, 85; H_2, 70; Ar, 300.

Kinetic parameters of the NO reduction are given in Table 1. An apparent activation

TABLE 1

Parameters of NO–H_2 Reaction

Pt Loading		Rate at 323 K nmol/(m²·s)[a]	Turnover frequency 1/ks	Apparent activation energy kJ/mol	$\frac{N_2}{N_2 + N_2O}$ %
wt%	μmol/m²[a]				
0.78	0.25	0.15	0.6	65.3	7.9
1.64	0.48	0.51	1.1	59.4	9.8
4.90	1.68	5.77	3.4	62.8	7.6
7.39	2.82(2.2)[b]	10.2	4.6	66.5	9.3
13.8	4.60(2.2)	15.7	7.1	63.6	9.1
23.1	12.3(2.2)	49.7	22.6	59.0	8.5

[a] m² of BET surface area.

[b] Numbers in parentheses show saturation concentration of Pt surface atoms.

energy, E, based on the Arrhenius equation, was calculated from the temperature dependence of the reaction rate

$$R(T) = r_0 \exp(-E/RT) \qquad (1)$$

where r_0 is a constant, T the absolute temperature, and R the gas constant. The activation energy remains rather constant at 62.8 kJ/mol within a standard deviation of ±3.1 kJ/mol. This deviation falls within the limits of our experimental error. A standard reaction rate per m^2 BET area was derived at 323 K, sometimes by interpolation, using Eq. (1). This rate is also listed in Table 1; it varies from 0.15 to 50 nmol/(m^2 (BET) · s) as the Pt loading increases from 0.78 to 23.1 wt% Pt. In Fig. 2, the rate is plotted versus Pt loading on a logarithmic scale to illustrate the concentration dependence more clearly. Table 1 shows also a turnover frequency, which is defined by the conversion rate of NO molecules per Pt site on the catalyst surface. The site density follows from the chemisorption of hydrogen and carbon monoxide (*2*). At lower concentrations each deposited Pt atom has to be counted as a surface atom, at higher concentrations the metal forms a saturation concentration of surface atoms at 2.2 μmol Pt/m^2 (BET). The turnover frequency shows a substantial increase with Pt concentration.

Diffusion hindrance is judged to be negligible. To avoid local overheating during the exothermic NO reduction, reaction rates were kept low. As Fig. 1 shows, several hours were usually needed to complete the reaction over small sample grains (size range 0.5–1.0 mm) (*2*).

It was observed previously at higher temperatures on Pt (*3*) and on Ru (*4*) that the product distribution resulting from NO reduction by hydrogen or ammonia is rather insensitive to a change in temperature within a certain temperature range. The same observation was made during this study. Averaged percentages of molecular nitrogen in the measured products containing nitrogen atoms are given in Table 1 for

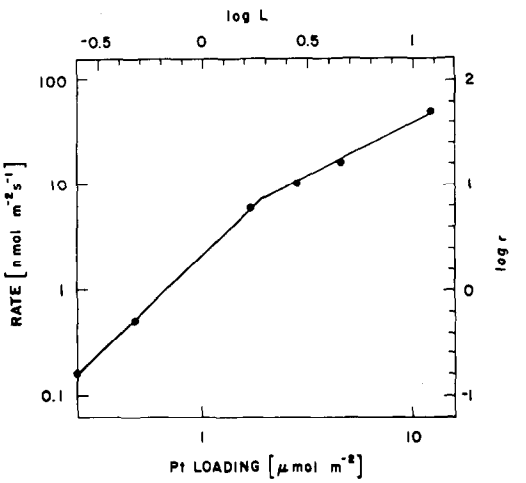

FIG. 2. Rate of NO reduction per m^2 (BET) at 323 K as a function of Pt loading.

each catalyst sample. An average N_2 percentage $N_2/(N_2 + N_2O) = 9\%$ (at about 323 K) shows that the formation of nitrogen molecules is a minor reaction path under our experimental conditions. Most of the nitric oxide is reduced to nitrous oxide. However, an N_2 percentage as high as 13% and as low as 3% was measured occasionally. An example of an exceptionally small N_2 percentage of 3.0% at 330 K (4.2% at 370 K) was observed at the lowest Pt loading (0.78 wt%) during the first reaction run. This percentage ultimately increased to 7.9% in subsequent runs. A concomitant increase in the reaction rate by a factor of 2.5 from 0.06 to 0.15 nmol/(m^2 (BET) · s) was measured. The two changes are assumed to be associated with the formation of Pt patches or clusters, as will be discussed below. Table 1 shows the data of the final run for this sample.

Table 2 shows an example of the product distribution on one of the Pt samples as a function of time. The reaction temperature was changed during this run from 273 to 297 K. The data show that formation of ammonia, if it exists under these conditions, is not an important side reaction. It follows from a comparison of the consumption of NO and the appearance of N_2O and N_2,

TABLE 2

Formation of Nitrous Oxide and Nitrogen during Reduction of Nitric Oxide over Pt at 23 wt%

T (K)	Time (s)	NO reacted (%)	N_2 produced (%)	N_2O produced (%)	$\frac{\Delta NO}{2(N_2 + N_2O)}$	$\frac{N_2}{N_2 + N_2O}$ (%)
273	1,800	7.5	0.25	4.05	0.87	5.8
	3,600	11.0	0.44	5.28	0.96	7.7
297	12,900	36.7	0.81	16.6	1.05	4.7
	15,000	40.7	1.51	21.1	0.90	6.7
	15,900	64.8	1.57	30.3	1.02	4.9
	16,800	79.1	2.59	35.6	1.04	7.3
	17,940	99.6	23.8	26.0	1.00	47.8

expressed by $\Delta NO/2\ (N_2O + N_2)$ in Table 2, that other nitrogen-containing products, such as ammonia, account for less than 10% and probably even for not more than 5% of the consumed nitric oxide under our experimental conditions.

The N_2 percentage, shown in the last column of Table 2, remains rather constant at $6.2 \pm 1.5\%$ until about 80% of the initial NO has been reduced. At this point the nitrogen percentage increases rapidly to 47.8%, which is the endpoint of the reaction based on the initial reactant mixture. This result is in agreement with earlier observations on Pt (*3*) and Ru (*4*). From those studies it was concluded that N_2 and N_2O are formed from adsorbed NO. The possibility of a readsorption of N_2O from the gas phase followed by a subsequent reduction or dissociation to nitrogen is contradicted by these and other experimental observations. The N_2O production indicates that in the presence of NO, nitrous oxide is precluded from occupying reaction sites. Once the NO is consumed, N_2O reduction is fast. The dissociation of N_2O was found to be extremely slow in the temperature range examined.

DISCUSSION

It should be stressed that the distribution of products N_2, N_2O, and NH_3 depends on the reaction conditions. In the presence of many metals and metal oxides, the appearance of N_2O as an important reduction or dissociation product has been established by numerous investigations. However it has been found repeatedly at very low pressures on various single crystal faces of Pt that NH_3 can be an important product, N_2O a negligible product (*5–8*). Differences in the product distribution are explained by the fact that low coverage of Pt by NO and hydrogen favors the dissociation of NO on Pt (*5, 6, 8*) and leads to a preferential pairing of N atoms. At higher NO coverage the fraction of dissociated NO molecules is very small and a pairing between N surface atoms has a low probability. The production of negligible amounts of ammonia under our experimental conditions can be explained the same way because the ammonia is presumably produced by the addition of hydrogen atoms to N atoms derived from NO dissociation. At low NO pressures and excess hydrogen, ammonia can be a major product (*5, 6, 8*). Lowering of the reaction temperature (*6*) or of the H_2/NO ratio (*8*) suppresses the formation of ammonia.

It is of interest to evaluate a theoretical site density from the transition state theory for comparison with the density of chemisorption sites. A theoretical site density, which depends strongly on the reaction mechanism, can be calculated according to the classification of reaction mechanisms described by Maatman (*9*). Agreement between a measured and a theoretical site

density does not provide conclusive proof that a reaction is governed by a certain mechanism. A high degree of disagreement, however, can be used to reject a specific reaction mechanism as the rate-determining step. In brief, there are four reaction mechanisms of possible relevance in the catalytic reduction of NO by hydrogen (*9*): case 1, a zero-order reaction based on a single reactant or slow product desorption; case 2, the Rideal–Eley mechanism; case 3, the Langmuir–Hinshelwood mechanism; case 4, dissociation, requiring dual sites. The equations for these models, taken from Maatman (*9*) and the notation used are given in the appendix. Using the measured activation energy and the specific reaction rate at 323 K (Table 1), ranges of site densities, calculated for different reaction mechanisms from Eqs. (2)–(5), are given in Table 3. These densities can be compared with the site-density range derived from hydrogen chemisorption, which is also listed in Table 3.

In case of the Langmuir–Hinshelwood mechanism, an activation energy $E' = 35$ kJ/mol (*10*) is assumed for the dissociation of hydrogen molecules on a Pt surface. The calculated value c_s^2/L (Eq. 4) is a lower limit of the reaction-site density L, since L is always larger than the density of vacant reaction sites c_s. From adsorption isotherms of NO on oxidized and reduced Pt (*11*, *12*) it can be estimated that, at 323 K and 13.3 kPa (100 Torr), the density of empty sites c_s falls in the range from 0.3 to 0.8 L. Therefore L could exceed the basic value c_s^2/L, given in Table 3, by one order of magnitude. As pointed out by Maatman (*9*), a calculated L value is unacceptable if it is outside of the 10^{16}–$10^{21}/m^2$ range. On this basis the general Langmuir–Hinshelwood mechanism (case 3) as well as the Rideal–Eley mechanism (case 2) have to be rejected as the rate-determining step.

On the other hand, case 1, based on a slow desorption step, yields a very small reaction site density requiring that only one out of 10^5 hydrogen-adsorption sites is active as a reaction site. This site density appears to be too small for a realistic model.

TABLE 3

Site Density Based on Various Kinetic Models

Case	Unit of site density	Site density per m^2 (BET)
1 (Eq. 2)	L	2×10^{11}–5×10^{13}
2 (Eq. 3)	L	2×10^{21}–6×10^{23}
3 (Eq. 4)	$L > c_s^2/L$	3×10^{28}–8×10^{30}
4 (Eq. 5)	$L > c_s$	2×10^{16}–6×10^{18}
From chemisorption		2×10^{17}–2×10^{18}

Dissociation of NO as the rate-determining step (case 4) yields a calculated site density c_s which in this particular case represents the density of bare dual sites. This density is expected to be by about one order of magnitude smaller than the reaction-site density (*9*). Table 4 shows the c_s value and the chemisorption-site density for each of the catalysts tested. At lower Pt concentrations the calculated density for bare dual sites, c_s, and the chemisorption-site density are compatible. At higher Pt concentrations the c_s values appear to be too large, but they are still acceptable within the error margin. A lowering of E by only 7 kJ/mol (1.5 kcal/mol), for example, lowers c_s by a factor of 10. According to Maatman (*9*) an agreement of theoretical and experimental site densities within the same order of magnitude is entirely satisfactory. Under this consideration the dissociation model is acceptable, while the other reaction mechanisms, discussed above, are not.

The dissociation of NO as the rate-determining step is also plausible from other considerations. It follows from desorption studies on Pt black (*11*) and on the (111) surface of Pt single crystals (*12*) and also from an investigation by photoelectron spectroscopy (*5*) that NO is chemisorbed on Pt mainly nondissociatively. Furthermore, the measured activation energy of 63 kJ/mol falls within the range from 55 to 85

TABLE 4

Experimental Site Density and Site Density Calculated from Dissociation Model (Eq. 5)

Pt Loading μmol/m^2 (BET)	Site density 10^{18} per m^2 (BET)	
	Calculated	Measured[a]
0.25	0.05	0.15
0.48	0.02	0.29
1.68	0.78	1.01
2.82	5.44	1.32
4.60	2.86	1.32
12.3	1.63	1.32

[a] From chemisorption of H_2 and CO.

kJ/mol which has been derived for the dissociation process of NO on Pt (*13–15*). Dissociation as the rate-determining step is also supported by conclusions reached from adsorption characteristics of NO and H_2 on single crystals of Pt (*6, 8*). The dissociation of hydrogen is considerably faster than that of NO and requires a much lower activation energy, as mentioned above. The curves in Fig. 1 suggest that the NO reduction is independent of pressure. It should be noted, however, that a batch reactor is inherently a poor instrument for measuring a reaction order. A reaction order of $\frac{1}{2}$, underlying the dissociation mechanism, is not contradicted by the experiment, as a closer inspection of the rate data shows.

The kinetics of the NO–H_2 reaction over Pt and over Rh, supported on γ-alumina, show certain similarities at lower metal loading. For example, the apparent activation energy over the two metals is the same within the experimental error (Rh 62.8, Pt 61.3 kJ/mol), and molecular nitrogen accounts for only 8–10% of the nitrogen-containing products in both cases. Furthermore, the dispersed phase reaches a saturation point at practically the same metal loading Rh 2.5, Pt 2.2 μmol/m^2 (BET). Both metals show a substantial increase in turnover frequency beyond the saturation point of the dispersed phase. At this concentration the metals cover only about 10% of the available alumina surface. On the other hand, the Pt turnover frequency at a given temperature exceeds that of Rh by two orders of magnitude. Since the apparent activation energy is the same for both metals, the difference in turnover frequency appears to be associated primarily with the geometrical surface structure of the catalysts. It is plausible, for example, that Rh, compared to Pt, remains oxidized to a larger degree under the conditions of the rate measurements and thus displays fewer active reaction sites. The higher affinity of Rh for oxygen has been shown recently by reduction studies (*1, 2*) and by electron microscopy (*16*) on highly dispersed Pt and Rh. Consistent with this concept is the fact that NO chemisorbs to a smaller degree on an oxidized surface than on a reduced surface. This adsorption characteristic has been observed on Pt (*11*) and on different oxides of Cr (*17*) and of Fe (*18*). It should be noted that at higher metal loadings of Pt and Rh some of the kinetic parameters, such as product distribution and apparent activation energy, show significant differences for Pt and Rh.

The striking increase in turnover frequency beyond the saturation concentration of the dispersed Pt phase is an experimental fact, which has also been observed in the case of Rh (*1*). An explanation for this activity increase can be based on the growth pattern of Pt clusters as a function of metal loading. It appears that at low surface coverage, Pt consists to a considerable degree of isolated atoms. Reduction of NO on a single site has to be based on a series of consecutive steps: chemisorption of NO, followed by the reaction of another NO molecule from the gas phase with the adsorbed nitrogen atom, which becomes dissociated from its oxygen atom resulting in the formation of N_2O. Combination of the residual oxygen atom with a hydrogen molecule closes the cycle. This Rideal–Eley mechanism, however, has to be rejected on the basis of the calculations dis-

cussed above, and thus does not add significantly to the reduction of NO over Pt or Rh (*1*).

Even isolated dual sites cannot be expected to offer an optimum configuration of sites for a transition complex, since the NO reduction requires at least two nitric oxide molecules and two hydrogen atoms. It can be conjectured that a cluster of at least five or six atoms is needed to form the most favorable configuration of the reactants in a surface complex. At the lowest Pt concentration (0.78 wt%) after treatment in oxygen at 775 K for 3 hr, or in hydrogen at 575 K for the same time, Pt particles were not visible by transmission electron microscopy (*2*). Under the conditions of the sample preparations the particles, observed by TEM, remain very small and do not exceed 3 nm, even at the highest Pt concentration (23 wt%) (*2*). Clusters which contain the minimum number of Pt atoms required for the optimum turnover frequency, as suggested above, may well be formed in an ever increasing number beyond the saturation concentration of the dispersed Pt phase.

The presence of isolated Pt atoms is supported by the observation of a reactivity change at the lowest metal loading. During the initial runs at 0.78 wt% of Pt, the percentage of $N_2/(N_2 + N_2O)$ increased gradually from 3 to 8%, while the reaction rate more than doubled during the same time. This observation suggests that some of the Pt atoms coalesce under the reaction conditions. An increase in the average size of the Pt clusters or patches is expected to facilitate the formation of a favorable configuration of sites for formation of the surface complex and for the continued reduction of adsorbed N_2O to N_2, mentioned above.

Furthermore, it was demonstrated in a series of experiments by temperature-programmed reduction (*2*) that reduction of Pt in the dispersed phase requires higher temperatures than does the reduction of Pt particulates. This result indicates that Pt in the dispersed phase interacts more strongly with the alumina support than does the particulate phase. The higher oxidation state of Pt in the dispersed phase is expected to result in a lower turnover frequency, as compared to a lower oxidation state of Pt in the particulate phase.

It is of interest to examine catalyst efficiency as a function of Pt loading. Catalyst efficiency is best described by the reaction rate per total number of Pt atoms, in contrast to turnover frequency, which is based on Pt surface atoms. Below the saturation concentration of the dispersed phase at 2.2 μmol Pt/m^2 (BET) both units are indistinguishable and show a substantial increase with Pt loading (Table 1). After the phase change the turnover frequency continues to increase, but more Pt atoms are now located inside of particles and clusters, unaccessible as catalytic sites, and counteract the advantage of increased turnover frequency. As a result the catalyst efficiency does not benefit from an increase in Pt loading above about 5 wt%.

These considerations lead to the conclusion that the increase in reaction rate above the saturation concentration of Pt in the dispersed phase does not require a change in the basic reaction mechanism, but can be explained by a rearrangement of Pt atoms into geometrical configurations better suited for the accomodation of the reactants. Because of the uncertainty associated with the arrangement of reactants in a surface complex, the concept of equivalent chemisorption and reaction sites on Pt requires further refinement. Chemisorption, however, establishes an upper limit of the reaction-site density.

APPENDIX: NOTATION

Density of reaction sites: L (sites cm^{-2})
Unoccupied sites: c_s (sites cm^{-2})
Number of active sites adjacent to a reaction site: s_a
Reaction rate: $v(T)$ (molecules cm^{-2} s^{-1})
Temperature: T(K)
Activation energy: E (J mol^{-1})

Gas density: c_g (molecules cm^{-3})
$F_{tr} = (2\pi\, mkT)^{3/2}/h^3$
$F_{rot} = (8\pi\, ^2IkT)/h^2$
Avogadro constant: $A = 6.02 \times 10^{23}$ (molecules mol^{-1})
Mass of NO molecule: $m = 30/A$ (g)
Mass of H_2 molecule: $m' = 2/A$ (g)
NO moment of inertia: $I = 16.3 \cdot 10^{-40}$ ($g \cdot cm^2$)
H_2 moment of inertia: $I' = 0.47 \cdot 10^{-40}$ ($g \cdot cm^2$)
Boltzmann constant: $k = 1.38 \cdot 10^{-16}$ (erg K^{-1})
Pianck constant: $h = 6.63 \cdot 10^{-27}$ (erg · s)
Gas constant: $R = 8.31$ (J K^{-1} mol^{-1})

$$L = ve^{E/RT}/(kT/h) \tag{2}$$

$$L = vF_{tr}F_{rot}e^{E/RT}/(c_gkT/h) \tag{3}$$

$$c_s^2/L = 2vF_{tr}F'_{tr}F_{rot}F'_{rot}e^{E/RT}/s_ac_gc'_g(kT/h) \tag{4}$$

$$c_s = v(F_{tr}F_{rot})^{1/2}e^{E/RT}/c_g^{1/2}(kT/h). \tag{5}$$

REFERENCES

1. Yao, H. C., Yao, Y.-F. Yu, and Otto, K. *J. Catal.* **56,** 21 (1979).
2. Yao, H. C., Sieg, M., and Plummer, H. K., Jr., *J. Catal.* **59,** 365 (1979).
3. Otto, K., Shelef, M., and Kummer, J. T., *J. Phys. Chem.* **74,** 2690 (1970).
4. Otto, K., and Shelef, M., *Z. Phys. Chem. NF* **85,** 308 (1973).
5. Bonzel, H. P., and Pirug, G., *Surface Sci.* **62,** 45 (1977).
6. Pirug, G., and Bonzel, H. P., *J. Catal.* **50,** 64 (1977).
7. Lambert, R. M., and Comrie, C. M., *Surface Sci.* **46,** 61 (1974).
8. Gland, J. L., Sexton, B. A., and Kollin, E. B., Research Report GMR-3198 PCP-120, January 1980, General Motors, Warren, Michigan.
9. Maatman, R. W., *J. Catal.* **43,** 1 (1976).
10. Bond, G. C., "Catalysis by Metals," p. 171. Academic Press, New York, 1962.
11. Otto, K., and Shelef, M., *J. Catal.* **29,** 138 (1973).
12. Gland, J. L., and Sexton, B. A., Research Report GMR-3081 PCP-109, September 1979, General Motors, Warren, Michigan.
13. Green, T. E., and Hinshelwood, C. N., *J. Chem. Soc.* **129,** 1709 (1926).
14. Winter, E. R. S., *J. Catal.* **22,** 158 (1971).
15. Shelef, M., Otto, K., and Gandhi, H., *Atm. Environ.* **3,** 107 (1969).
16. Chen, M., Wang, T., and Schmidt, L. D., *J. Catal.* **60,** 356 (1979).
17. Otto, K., and Shelef, M., *J. Catal.* **14,** 226 (1969).
18. Otto, K., and Shelef, M., *J. Catal.* **18,** 184 (1970).